energies

MDPI

Article

Combustion of Polycarbonate and Polycarbonate–Carbon Nanotube Composites Using Fluidized Bed Technology

Lakhdar Sidi Salah [1,2], Gabriela Berkowicz-Płatek [3,4], Witold Żukowski [3,*], Yann Danlée [2], Isabelle Huynen [2], Kinga Wencel [5,6], Jan Wrona [5] and Dawid Taler [5]

1 Laboratory of Coatings, Materials and Environment, M'Hamed Bougara University, Boumerdes 35000, Algeria; l.sidisalah@univ-boumerdes.dz
2 ICTEAM Institute, Université Catholique de Louvain, 1348 Louvain-la-Neuve, Belgium; yann.danlee@uclouvain.be (Y.D.); isabelle.huynen@uclouvain.be (I.H.)
3 Faculty of Chemical Engineering and Technology, Cracow University of Technology, Warszawska 24, 31-155 Cracow, Poland; gabriela.berkowicz@pk.edu.pl
4 Interdisciplinary Center for Circular Economy, Cracow University of Technology, Warszawska 24, 31-155 Cracow, Poland
5 Faculty of Environmental Engineering and Energy, Cracow University of Technology, Warszawska 24, 31-155 Cracow, Poland; kinga.wencel@pk.edu.pl (K.W.); jan.wrona@pk.edu.pl (J.W.); dawid.taler@pk.edu.pl (D.T.)
6 Doctoral School, Cracow University of Technology, Warszawska 24, 31-155 Cracow, Poland
* Correspondence: witold.zukowski@pk.edu.pl

Abstract: This study investigates the combustion behavior of polycarbonate (PC) and polycarbonate–carbon nanotube (PC-CNT) composites in fluidized bed reactors. The primary objective was to evaluate the influence of carbon nanotubes (CNTs) on the thermal stability and combustion efficiency of PC. Simultaneous thermogravimetric and differential scanning calorimetry (TG-DSC) analyses were conducted under both air and oxygen-deficient conditions to assess decomposition temperature ranges and energetic effects. Additionally, a simultaneous TG-DSC analysis of the samples' decomposition in a 2 vol.% O_2 atmosphere was carried out to simulate adverse combustion conditions that may occur in some combustion technologies, such as the accumulation of degraded material on the grate. Combustion experiments were performed in inert and catalytic fluidized beds, the latter incorporating Fe_2O_3-coated cenospheres to enhance catalytic activity. The results demonstrated that the presence of CNTs alters the combustion mechanism, reducing energy release in the initial degradation stage while significantly intensifying exothermic effects in subsequent stages. Under oxygen-deficient conditions, both PC and PC-CNT required higher temperatures and extended times for complete decomposition. The catalytic fluidized bed markedly improved combustion efficiency at lower temperatures, achieving up to 90% conversion at 550 °C, compared to inert beds that required 750 °C for similar efficiency.

Keywords: polycarbonate; carbon nanotubes; combustion; fluidized bed

check for updates

Academic Editors: Franz Winter, Rafał Kobyłecki, Artur Blaszczuk and Hairui Yang

Received: 17 February 2025
Revised: 27 March 2025
Accepted: 2 April 2025
Published: 4 April 2025

Citation: Salah, L.S.; Berkowicz-Płatek, G.; Żukowski, W.; Danlée, Y.; Huynen, I.; Wencel, K.; Wrona, J.; Taler, D. Combustion of Polycarbonate and Polycarbonate–Carbon Nanotube Composites Using Fluidized Bed Technology. *Energies* **2025**, *18*, 1833. https://doi.org/10.3390/en18071833

Copyright: © 2025 by the authors. Licensee MDPI, Basel, Switzerland. This article is an open access article distributed under the terms and conditions of the Creative Commons Attribution (CC BY) license (https://creativecommons.org/licenses/by/4.0/).

1. Introduction

Polycarbonate (PC), an amorphous thermoplastic polymer, is widely recognized for its excellent optical transparency, high impact resistance, and thermal stability [1,2]. This synthetic thermoplastic polyester has an average high molecular weight conferring fair stability to aging [3]. These characteristics make PC an ideal candidate for various advanced applications, including those in the field of nanocomposites [4]. It is mainly produced by the polycondensation of Bisphenol A with phosgene [5]. It contains carbonate groups, making

it an oxygen-containing polymer as the mass fraction of C/O = 0.189. PC is characterized by the presence of rigid aromatic functionalities in the polymer backbone; this characteristic imparts outstanding physical and chemical properties. It starts to decompose at 433 °C; however, the destructive process of PC is mostly efficient when a temperature of about 550 °C is reached [6–8].

The extensive production of PC worldwide incites academic researchers to valorize its mechanical, electrical, and electromagnetic performances by introducing low-volume fractions of nanoparticles such as multi-walled carbon nanotubes (MWCNTs). These nanocharges essentially consist of rolling multiple cylinders made of a graphene tube on a common central hollow with a spacing of 0.34 to 0.39 nm between the layers [9]. MWCNTs allow the reinforcement of the host polymer as well as the formation of new hybrid systems that are actively used as microwave shielding devices to reduce electromagnetic pollution [10]. With more than 350 million tons of plastic produced in 2018 and less than 15% collected for recycling globally, the amount of plastic waste being released into the environment is increasing exponentially [11–13]. The successive processing of PC and PC-CNT blend up to twenty cycles leads to a decrease in mechanical and rheological properties of PC-CNT compared to neat resin. This decrease is attributed to chain scission and molecular weight reduction from the repeated high shear and thermal stresses in the recycling process. It was concluded that mechanical recycling of filled PC-CNT should be avoided as nanocomposites lose the properties that lead to them being applied in industry in the first place. When mechanical recycling ceases to be beneficial, thermal methods should be taken into consideration, specifically combustion and feedstock recycling.

PC has an excellent resistance to fatigue and high chemical stability [14,15]. Thus, its presence in the environment may make its degradation resistant for many years. Recycling becomes a great challenge involving the implantation of infrastructures for the chemical recycling of most commodity materials instead of landfilling plastics into the soil. The upcycling of a polymer consists of its selective conversion into higher-value chemicals or materials which allows for a significant reduction in the use of fossil fuels, the recovery of monomers or useful building blocks for subsequent polymerization, energy savings, and a reduction in the amount of plastics in the environment, which also generates an economic benefit [16,17]. Combustion is a high-temperature oxidation process. In the process, the compound is destroyed with the formation of new substances. The end products for the complete production of compounds containing carbon, hydrogen, and oxygen atoms are carbon dioxide and water vapor [18]. In fact, each type of combustion is a very complex process with a series of intermediate stages, and complete combustion products are not always produced in the first combustion zone. The most harmful products of incomplete combustion, primarily carbon monoxide and volatile organic compounds, must be oxidized in the next combustion zone. This applies to industrial incinerators and waste incinerators [19]. Fluidized bed (FB) reactors are very favorable equipment for thermal heat energy recovery from various types of waste [20]. In an industrial fluidized bed reactor, a chemically inert or active layer is fluidized by air, and fuels are mixed with the fluidized bed and the oxygen source supplied by air. If the combustion materials considered are relatively resistant to decomposition and therefore hardly oxidizing, the hot particles in the fluidized bed heat them and accelerate their thermal decomposition [21]. Połomska et al. [8] have investigated the co-combustion of polycarbonate with propane in the presence of air in the fluidized bed reactor, filled with quartz sand or limestone, from visual observation and quantitative analysis; the authors suggested limestone as a fluidized reactor bed for the combustion of PC while a higher growth of temperature in the reactor freeboard space and some diffusive flames were provided by the higher hydrodynamic mixing of the fuels with air provided by limestone FB. The thermal degradation of PC has

also been analyzed with the help of TGA-FTIR analysis by Esin Apaydin-Varol et al. in work [22], but so far these have only been the qualitative analyses of bands in the spectrum of the mixture of products [23]. However, an appropriately selected analytical method with the help of FTIR may also allow a quantitative evaluation of the products of the process, and is the objective of the present study. Studies conducted in a thermogravimetric analyzer provide valuable information about the thermal properties of materials and can be useful in preliminary research, but they are conducted on a small scale and therefore, may not reflect the behavior of materials in industrial reactors.

In the face of escalating climate challenges, a comprehensive approach to the production of new materials is becoming increasingly important. It is crucial not only to ensure the efficient use of raw materials and minimize environmental impact during their acquisition and processing but also to consider the ultimate disposal of products. The long-term utility of materials does not end with their use. An equally important aspect is planning for their life after the end of use. This strategy, known as the "cradle to grave" approach, assumes the responsibility of producers not only for the quality and functionality of products but also for their future fate. Incorporating the disposal stage into the entire product lifecycle is fundamental for sustainable development. This requires innovation in product design so that they are easier to recycle or biodegrade.

Laboratory-scale studies of PC–CNT composite combustion focus on evaluating material flammability, identifying combustion mechanisms, and determining the total heat released during the process [24]. The behavior of PC–CNT composites under combustion conditions similar to those found in commercial waste incineration plants was presented in ref. [25]. The experimental approach was based on a standard fluidized bed with sand as the bed material. The use of sand required a high volumetric air flow rate (130 dm^3/min for a reactor with a diameter of approximately 10 cm). To achieve sufficiently low concentrations of pollutants in the flue gas, the authors implemented multistage secondary air injection and the electrical preheating of the process gases. Another unfavorable phenomenon, resulting from Archimedes' principle, is the entrainment of PC particles above the fluidized bed. The density of a fluidized bed made of sand is about 1.5 g/cm^3 [26] and the density of polycarbonate is about 1.2 g/cm^3. Hence, in accordance with Archimedes' principle, polycarbonate will tend to rise to the surface of the fluidized bed. Połomska et al. used a transparent quartz reactor to enable the direct observation of diffusion flames above the sand-fluidized bed during the combustion of polycarbonate [8,27]. In a process organized in such a way that the combustion of gases evolved from PC occurs above the fluidized bed, the use of a catalytic fluidized material cannot provide the expected improvement in PC conversion.

Since the key challenge in fluidized bed combustion of polymeric materials lies in the proper localization of the combustion zone, it becomes essential to shift the combustion process into the fluidized bed, where more stable thermal and flow conditions exist. In this context, the application of cenospheres—hollow microspheres with a density below 1 g/cm^3—as bed material may fill a significant research gap and offer new possibilities for the efficient combustion of polycarbonate. This innovative approach using a low-density inert fluidized bed can also be extended to a catalytic fluidized bed, provided that an active catalytic layer is deposited onto the cenospheres. The proposed solution offers the potential to accomplish the following: (I) localization of the combustion of PC into the fluidized bed, (II) extension of the residence time of reactants, thereby improving combustion efficiency and potentially eliminating the need for additional post-combustion zones, which otherwise complicate the system design, and (III) facilitation of the reactor operation at a lower pressure drop due to the lower bulk density of cenospheres compared to sand.

2. Materials

Makrolon® OD2015 from Bayer AG (Leverkusen, Germany) polycarbonate was used as the polymer matrix. As conductive nanofillers, multi-walled carbon nanotubes NC7000 from NanoCyl SA (Sambreville, Belgium) were used. The nanotubes were produced by the catalytic chemical vapor deposition method. Their physical properties are reported in [28]. The densities of PC and MWCNTs are 1.19 g/cm^3 and 1.75 g/cm^3, respectively. CNTs were added with a 5% weight concentration. Such a CNT content in PC allows for achieving a balance between obtaining functional electrical properties and maintaining the processability and mechanical integrity of the material [29]. It was proved in [28] that the composite PC—5 wt.% CNT reached the best absorption index following the Rozanov formalism with the implementation process by hot extrusion. The composite compounds were melt-blended at 280 °C for 5 min at 150 RPM in a micro 15 DSM micro-compounder. Composite pellets were twice hot-pressed in Fontijne press under 290 °C, 7.5 T, and 2.5 min to produce films with 140 µm thickness.

Cenospheres were provided by the Połaniec power plant in Poland. Completely intact, whole spheres without any damage or perforations were isolated from others by floating on the surface of the water. Cenospheres are hollow aluminosilicate microspheres, having thermal resistance of up to 1400 °C and a mechanical strength of up to 210–350 kg/cm^2. The low density and good sphericity make this material fluidized at a low minimum fluidization velocity (at 700 °C, minimum fluidization velocity is 1.0 cm/s, and terminal fluidization velocity is 78.1 cm/s) as reported in [22]. The catalytic Fe_2O_3 cenospheres contained 12% mass of oxide and were obtained by covering the cenospheres with iron during the process of thermal decomposition of $Fe(CO)_5$ at 180 °C, and then oxidized by air according to the procedure described in [30].

For STA (simultaneous thermal analysis) and FTIR (Fourier-Transform Infrared Spectroscopy) analyses, two types of gases were utilized, both sourced from Air Products. The first gas was nitrogen, of the 'Premium' grade, with a high purity level of 99.995%. The second gas was oxygen, designated as 'Ultra-Pure', also notable for its high purity, measured at 99.999%. The combustion tests were conducted in a fluidized bed using a stream of atmospheric air.

3. Methods

The preliminary studies of simultaneous thermal analysis (STA), incorporating concurrent thermogravimetry (TG) and differential scanning calorimetry (DSC) measurements, were conducted using the STA 449 F3 Jupiter Analyzer from Netzsch (Selb, Germany). The STA was performed in an atmosphere of 21% O_2 in the range of 50 to 1000 °C based on a dynamic temperature increase of 20 °C/min. The masses of the samples used for the STA were 9.86 and 6.63 mg, respectively, for PC and PC-CNT. The carrier gas containing 21% O_2 was obtained using flows of 100 mL/min of nitrogen and 26 mL/min of oxygen.

The primary combustion tests for the PC and PC-CNT blend films were conducted in a fluidized bed (FB) reactor, as depicted in the schematic arrangement presented in Figure 1. The quartz reactor, cylindrical in shape, stood vertically and had dimensions of 530 mm in length and a diameter of 96 mm. A ceramic heater surrounding the reactor was used to heat the fluidized bed. The thermocouple was installed at the bottom of the reactor. Additionally, the reactor was wrapped in mineral wool insulation to minimize heat exchange with the atmosphere. Fluidized beds were heated to 550, 600, 650, 750, and 850 °C. PC and PC-CNT samples with a mass of around 200 mg were loaded into the fluidized bed through the free space at the top of the reactor. Exhaust gases were continuously sampled from the top of the reactor and analyzed using an FTIR spectrometer (model DX-4000, GASMET Technologies Oy (Vantaa, Finland). The entire gas path between the reactor

and the analyzers was maintained at 180 °C to avoid the condensation of water and other components. The setup was equipped with a camera visualizing the surface of the fluidized and a cyclone, which was used to capture particles escaping outside the reactor.

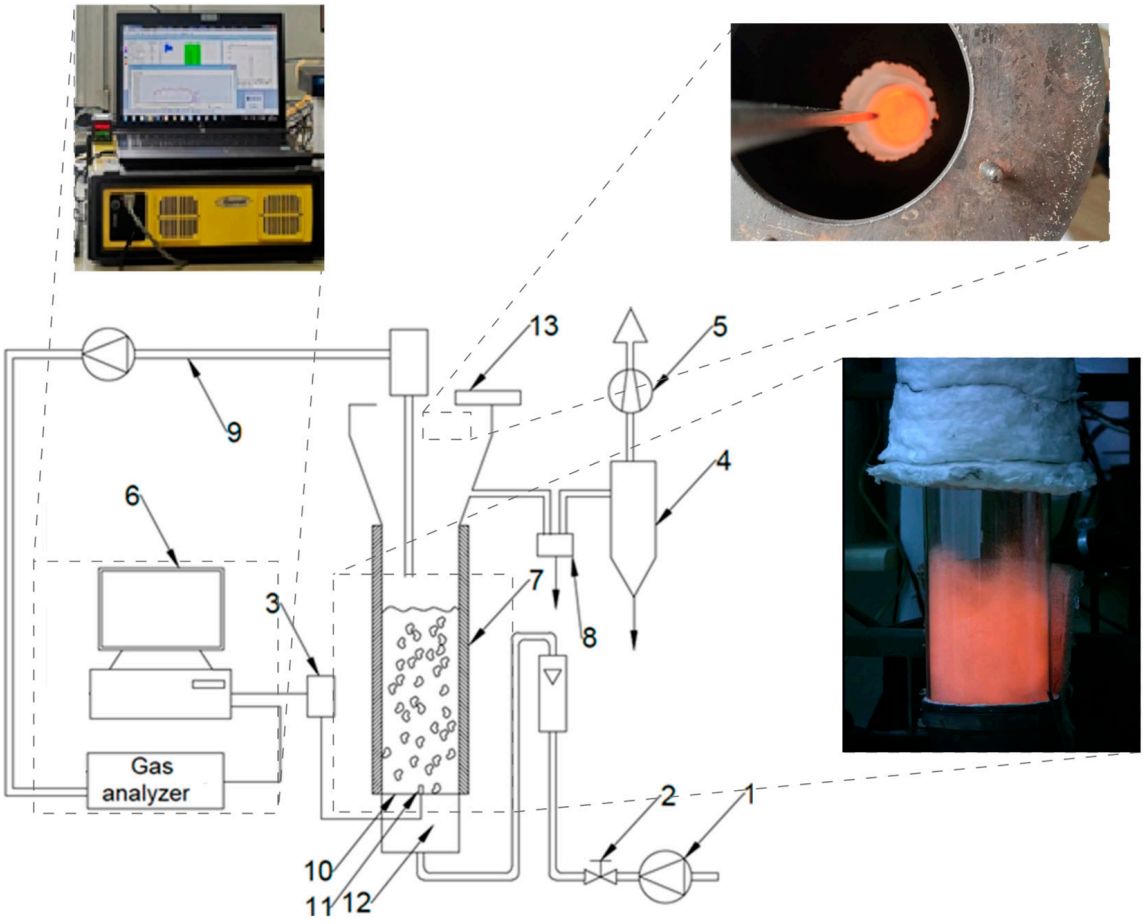

Figure 1. Experimental setup: 1—an; 2—gas valve; 3—A/D converter; 4—cyclone; 5—exhaust gases fan; 6—computer; 7—isolation; 8—settler; 9—gas pipe; 10—gas distributor; 11—thermocouple; 12—plenum chamber; 13—camera.

The FB reactor was filled with 300 g of inert or catalytic cenospheres. The bed materials were fluidized by 30 l/min of air getting in through the perforated Cr/Ni steel distributor on which the FB reactor was rested. The inert bed was formed from cenospheres with a grain size of 250–300 μm and a density of 845 kg/m^3. The catalytic bed was created using cenospheres of the same grain size, coated with a nanometric layer of Fe_2O_3. The Fe_2O_3 nanometric layer increased the grain mass by 12.5% but did not significantly affect its diameter (<1/250 diameter). The density of the Fe_2O_3-coated cenospheres was 951 kg/m^3. The fluidization behavior of materials used was described in the study [30], and based on experimentally determined minimum fluidization velocities, it was established that the Wen and Yu equation can be applied to calculate the minimum fluidization velocity (U_{mf}) at elevated temperatures for these materials. According to the Wen and Yu equation, for an equivalent diameter of 275 μm, densities of materials and the temperatures used for the combustion of PC and PC-CNT, the U_{mf} values of cenospheres, and Fe_2O_3-coated cenospheres were determined in Table 1.

Table 1. Fluidization velocities depending on bed temperature (U_{mf}—minimum fluidization velocity, cm/s; U—superficial gas velocity in the reactor, cm/s; U_{tr}—terminal velocity of particles, cm/s).

	Fluidized Bed							
	Cenospheres				Fe_2O_3 Cenospheres			
Bed Temp., °C	**U_{mf}, cm/s**	**U, cm/s**	**U/U_{mf}**	**U_{tr}, cm/s**	**U_{mf}, cm/s**	**U, cm/s**	**U/U_{mf}**	**U_{tr}, cm/s**
20	2.57	6.91	2.69	116.8	2.88	6.91	2.40	127.4
550	1.18	19.4	16.4	84.9	1.33	19.4	14.5	94.3
600	1.13	20.6	18.1	82.5	1.28	20.6	16.1	91.7
650	1.08	21.8	20.0	80.2	1.22	21.8	17.8	89.2
750	1.01	24.1	24.0	76.1	1.13	24.1	21.3	84.7
850	0.93	26.5	28.2	72.3	1.06	26.5	25.1	80.6

Within the assumed temperature range of 550 to 850 °C, the U_{mf} of the materials varied from 1.18 to 0.93 cm/s for inert cenospheres and from 1.33 to 1.06 cm/s for Fe_2O_3-coated cenospheres. The materials were fluidized using air at a constant volumetric flow rate of 30 dm^3/min. At this gas flow rate and for a reactor diameter of 9.6 cm, the U/U_{mf} ratio at room temperature was 2.69 for cenospheres and 2.40 for Fe_2O_3-coated cenospheres. This choice of U/U_{mf} ensured proper material mixing during the heating of fluidized beds. As the temperature increases, the superficial gas velocity in the reactor (U) also rises, reaching 26.4 cm/s at 850 °C. Simultaneously, according to calculations using the Wen and Yu equation, U_{mf} decreases—up to 2.5 times at 850 °C compared to U_{mf} at ambient temperature. As a result of these two changes, the U/U_{mf} ratio increases to 28.2 for cenospheres and 25.1 for Fe_2O_3-coated cenospheres at 850 °C. High U/U_{mf} values ensure significant bed turbulence, which enhances the oxidizer's accessibility to the combusted material, leading to the desired combustion efficiency. Despite some differences in bed fluidization behavior, the U/U_{mf} values at given temperatures remained comparable. At the highest temperature, the superficial gas velocity (U) is 2.7 to 3 times lower than the particle transport velocity (U_{tr}), preventing mass loss of the bed during the process.

4. Results

4.1. Simultaneous Thermal Analysis in Air and Oxygen-Poor Atmosphere

The results of the simultaneous thermal analysis (STA) presented in Figure 2 show the mass loss of samples (green TG curves) and the accompanying thermal effects (blue DSC curves) obtained for the PC (Figure 2a) and for the PC-CNT composite (Figure 2b). The registered DSC curves are net thermal effects of complex processes, some of which are certainly endothermic, and some are exothermic. From the DSC curve, the instantaneous and total net heat effects can be determined. Instantaneous Net Heat Effect—i.e., a temporary, resultant thermal effect that takes into account both the instantaneous course of endothermic and exothermic processes. In the graph, the values of this Instantaneous Net Heat Effect are represented by the DSC curve (in mW/mg). Total Net Heat Effect—the total resultant thermal effect (calculated on the basis of the selected temperature range) refers to the total thermal effect recorded by the DSC. In Figure 2, this effect is marked in the form of hatched fields and the numerical values (in J/g) of this effect are additionally placed on the DSC plot. By convention, positive heat effects are associated with exothermic processes, whereas negative values indicate endothermic processes.

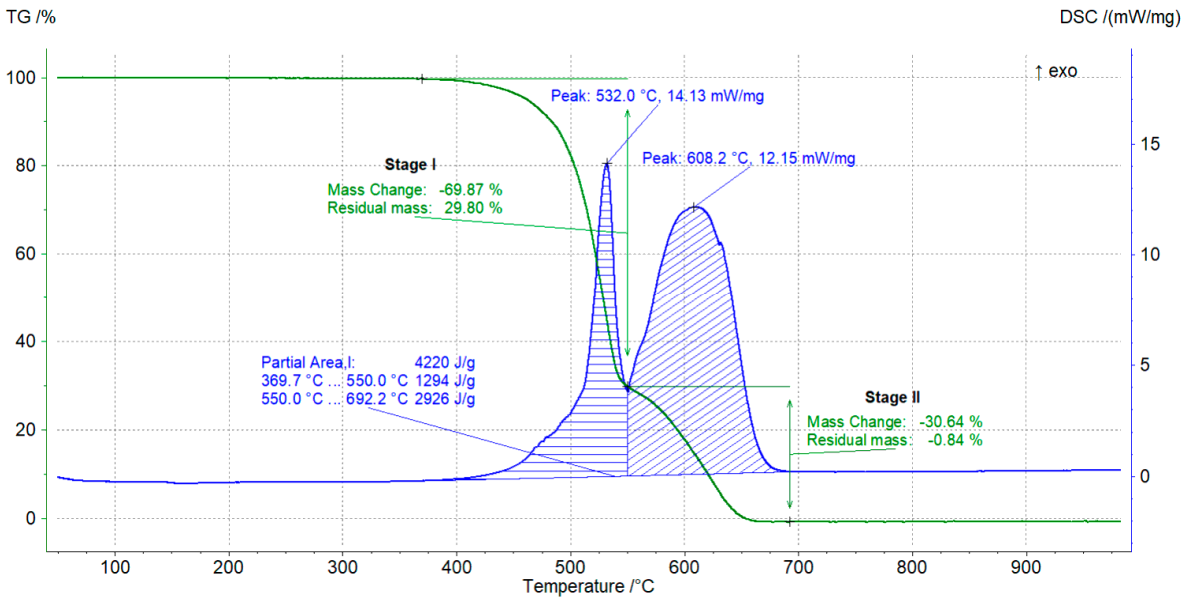

(**a**)

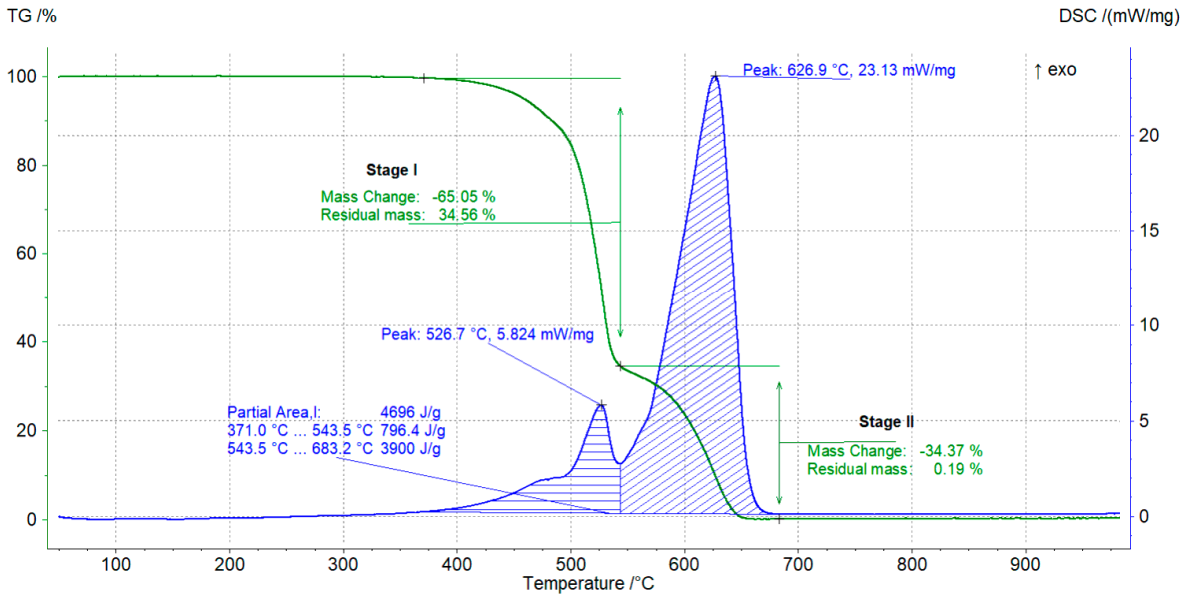

(**b**)

Figure 2. TG curves (in green) and DSC curves (in blue) obtained during the decomposition of (**a**) pure PC; (**b**) PC-CNT composite in an air atmosphere with a dynamic temperature increase of 20 °C/min.

Taking into account the shapes of the TG in the combustion of pure PC and PC-CNT composite, two stages of mass loss have been distinguished and are indicated in Figure 2. In the first stage of PC mass loss, the mass loss occurs in the range of 370–550 °C, amounting to 69.9% of its mass (Figure 2a). The maximum value of the instantaneous net heat effect was recorded at 532 °C, amounting to 14.1 mW/mg. As a result of the processes occurring in this stage, 1294 J/g was released. The second stage of PC mass loss was recorded in the temperature range of 550–692 °C, with the maximum instantaneous net heat effect at 608 °C amounting to 12.1 mW/mg. This stage involves a 30.6% mass loss and is associated with a total net heat effect of 2926 J/g. This corresponds to 70% of the total net heat effect recorded throughout the analysis. The high value of the total net heat effect in the second

stage indicates processes related to the combustion of the solid residue (char) after the polymer decomposition.

During the STA of PC-CNT combustion (Figure 2b), a similar two-phase arrangement was observed. The first stage of PC-CNT mass loss shows a lower degree (65% by mass) compared to pure PC. The lower values of the maximum instantaneous net heat effect (5.8 mW/mg) compared to PC (14.1 mW/mg), as well as the lower total net exothermic effect (796 J/g) compared to PC (1294 J/g) may indicate a modification of the polymer decomposition mechanism by the presence of CNT at first stage. This suggests that carbon nanotubes may influence the decomposition processes, potentially acting as barriers limiting the availability of polymer material for combustion reactions. Castillo et al. reported that the reduction in the change in heat capacity suggests that polymer chains are immobilized by the nanotubes, which can potentially affect the fire resistance properties [31]. It is stated in [32–35] that dispersed CNT enhances the flame retardancy of polymeric nanocomposites. Additionally, carbon nanotubes can reduce material flammability by forming a protective layer made up of a network of nanoparticles. This layer acts as a heat shield, re-emitting much of the incident radiation, which slows down polymer degradation and protects the matrix from oxygen radical attack. The main flame-retarding mechanism of nanofillers like carbon nanotubes in polymers is the formation of a char layer. The small filler-to-filler distance and large interface area of these carbon nanostructures help create a compact, dense char layer, which effectively slows heat transfer to combustible gases and restricts oxygen access to the underlying semi-pyrolyzed polymer [36].

The second stage of mass loss for the PC-CNT composite, amounting to 34.4%, occurred in the range of 543–682 °C, and is characterized by a higher maximum of instantaneous net heat effect (23.1 mW/mg) compared to pure PC (12.5 mW/mg) and higher total net heat effect (up to 3900 J/g) compared to pure PC (2926 J/g). This indicates a modification of the polymer decomposition mechanism by the presence of CNT also at the second stage. The presence of CNTs enhances thermal stability by promoting a gas barrier effect and increasing char residue at the second exothermic decomposition. Well-dispersed CNTs at elevated temperatures create a tortuous path for gas escape, delaying the exothermic process during decomposition. This results in higher thermal stability and increased mass of char residue [37].

In order to achieve the complete utilization of PC, the combustion process should be organized in such a way as to ensure the supply of a sufficiently large amount of oxygen. The use of grate technology may result in uneven distribution of waste on the grate. In places where the density of the material is higher, the supply of oxygen is limited. The molten polymer can form an additional coating that further reduces the supply of oxidizers. In the rotary kiln, the materials are turned. PC combustion in this technology may be associated with the formation of viscous layers that make it difficult for oxygen to reach the burned mass. One of the advantages of the combustion process in the fluidized bed technology over the above-mentioned technologies is intensive mixing, which allows for better contact of the oxidizer with the waste. In order to verify whether more efficient air distribution is necessary for the processing of PC and PC-CNT, in terms of the rate of mass loss and energy demand, additional tests were carried out and the 2% O_2 atmosphere was chosen to simulate oxygen-deficient conditions.

The results of the STA in the 2% O_2 atmosphere are shown in Figure 3a,b for the PC and PC-CNT, respectively. Limited oxygen access had no impact on the number of distinguished combustion stages but it did affect the magnitude of mass loss. In the first stage, the mass loss for PC increases from 69.8% in the air to 71.6% in the presence of 2 vol.% O_2. For PC-CNT, the mass loss rises from 65.0% in the air to 68.5% with 2 vol.% O_2. It may be surprising that the mass loss is greater in the oxygen-poorer atmosphere than in the

air. It is known from the scientific literature that in the process of combustion of polymer materials, a char layer can be formed on the surface of the material [38]. Especially for PC, which is aromatic, the formation of such a layer can be formed by the condensation of phenolic groups. Most likely, a more oxygen-rich atmosphere promotes faster formation of this char layer, preventing further reactions of the polymer with oxygen. A higher temperature is necessary for the char to react, and this is observed in the second phase.

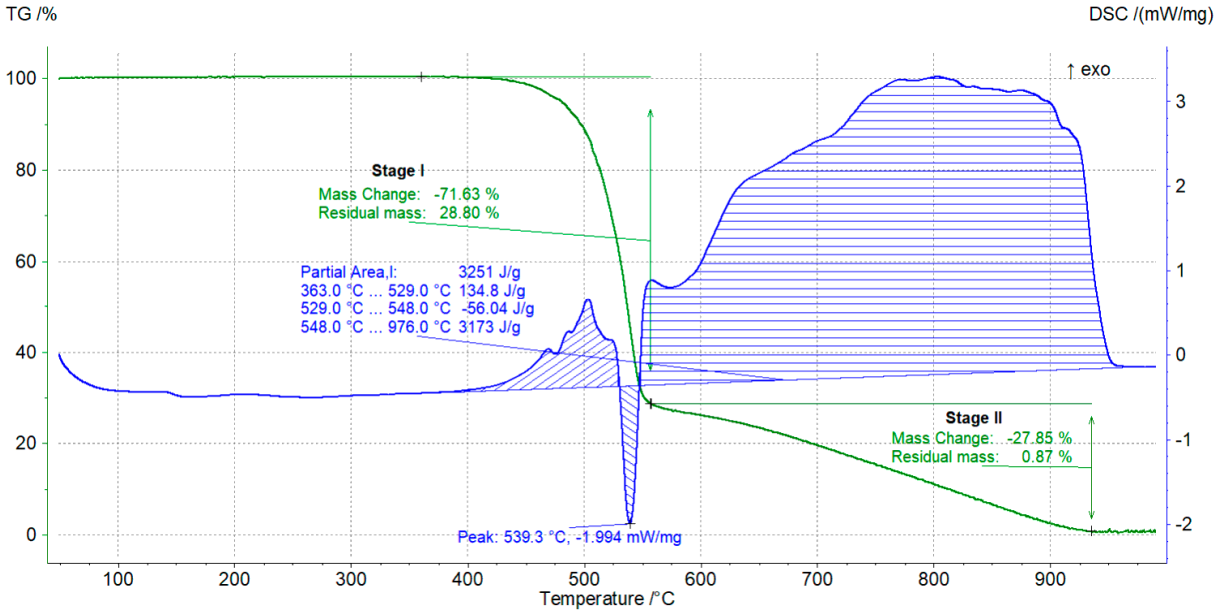

(**a**)

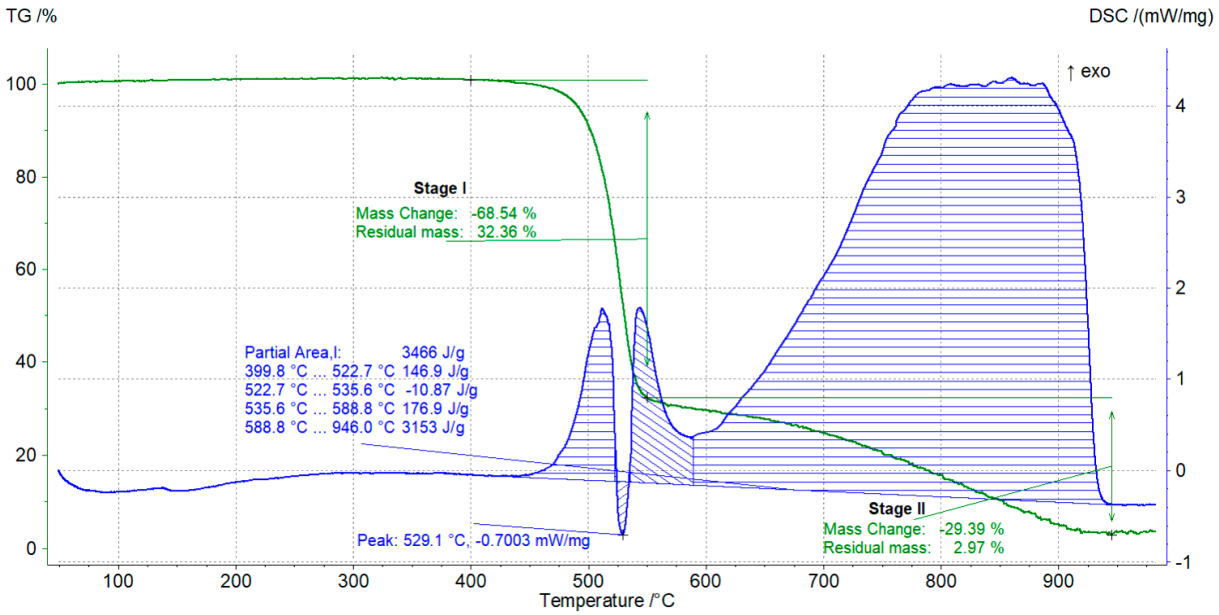

(**b**)

Figure 3. TG curves (in green) and DSC curves (in blue) obtained during the decomposition of (**a**) pure PC; (**b**) PC-CNT composite in an oxygen-deficient atmosphere (2%vol. O_2) with a dynamic temperature increase of 20 °C/min.

On the DSC curves, during the first stage of combustion in 2% O_2, it can be observed that the instantaneous net heat effect reaches its minimum, amounting to −2.0 mW/mg at 539 °C for PC and −0.7 mW/mg at 529 °C for PC-CNT. A temporary negative net effect results from

changes in the proportions of endothermic and exothermic complex processes, depending on which is dominant at a given moment. During the decomposition of PC in an atmosphere containing 2% O_2, multiple endothermic and exothermic processes occur simultaneously and overlap. Breaking the covalent bonds in polycarbonate requires an input of energy, making this process endothermic. At the same time, heterogeneous reactions involving oxygen, which are exothermic, take place on the polymer's surface. As the rate of sample mass loss increases, the oxygen deficit near the sample also increases. When the maximum mass loss rate is reached, the intense release of gaseous products limits oxygen diffusion to the sample surface, resulting in an instantaneous net heat effect of an endothermic nature.

In the second stage of PC decomposition in an atmosphere with 2 vol.% O_2, the processes associated with the burning of the solid residue slowed down so much that the PC sample burned out at 976 °C (Figure 3a), which is more than 283 °C higher than in the combustion process in an atmosphere with 21 vol.% O_2 (Figure 2a). A similar trend was observed for the PC-CNT composite, which burned out at approximately 946 °C under limited oxygen conditions compared to around 683 °C in air. The total net heat effects of PC and PC-CNT combustion in an atmosphere with 2 vol.% O_2 are approximately 1000 J/g lower than for combustion of these samples occurring in an air atmosphere, and amount to 3521 J/g and 3466 J/g for PC and PC-CNT, respectively.

Based on the instantaneous net heat effects recorded in a 2% O_2 atmosphere (Figure 3), it can be concluded that the presence of CNTs clearly limits flammability, particularly in the 570–740 °C range, which appears to be critical during the fire development stage. On the other hand, under conditions of full oxygen availability (21% O_2, Figure 2), CNTs behaved as an additional fuel, increasing the exothermic effect in stage 2 and not contributing to flammability reduction.

The STA results indicated that, under local oxygen deficit conditions, the decomposition of PC and PC-CNT would require significantly more time and higher temperatures, emphasizing the importance of ensuring a good supply of the oxidizing agent to maintain combustion efficiency. This can be achieved by fluidized bed technology, where intensive mixing in the fluidized bed allows for uniform oxygen delivery to the degrading material. Taking into account the maximum loss rates of the second stage of PC and PC-CNT decomposition in the air (Figure 2), it was established that the inert fluidized bed in which the process of thermal utilization of these materials will be tested must be heated to at least 650 °C to ensure effective decomposition of these materials.

4.2. Fluidized Bed Combustion of PC and PC-CNT

The chemical analysis of the combustion process of PC and PC-CNT in a fluidized bed was based on the FTIR spectra of the gaseous product mixture. The FTIR spectra were recorded every 7–8 s in the range of 900–4000 cm^{-1}. Each molecule in the gaseous mixture has its own characteristic IR spectrum, which serves as its fingerprint. In comparison to the IR spectra of solids and liquids, the spectra of gaseous components are much clearer and more accurate, making not only qualitative but also quantitative analysis possible. The quantities of individual components in the product mixture were determined based on reference spectra. The chemical results of experimental studies on PC and PC-CNT combustion in inert and catalytic fluidized beds are presented in Figures 4 and 5, respectively. They consist of four charts, labeled A to D. Chart A illustrates the conversion rate of polymeric carbon into the main combustion products—specifically CO2, CO, and organic compounds, as influenced by temperature and the type of raw material used. Chart B depicts the distribution of organic products into aromatic, aliphatic, and oxygenated derivatives. Charts C and D, respectively, show the proportions of individual aromatic and aliphatic products, respectively.

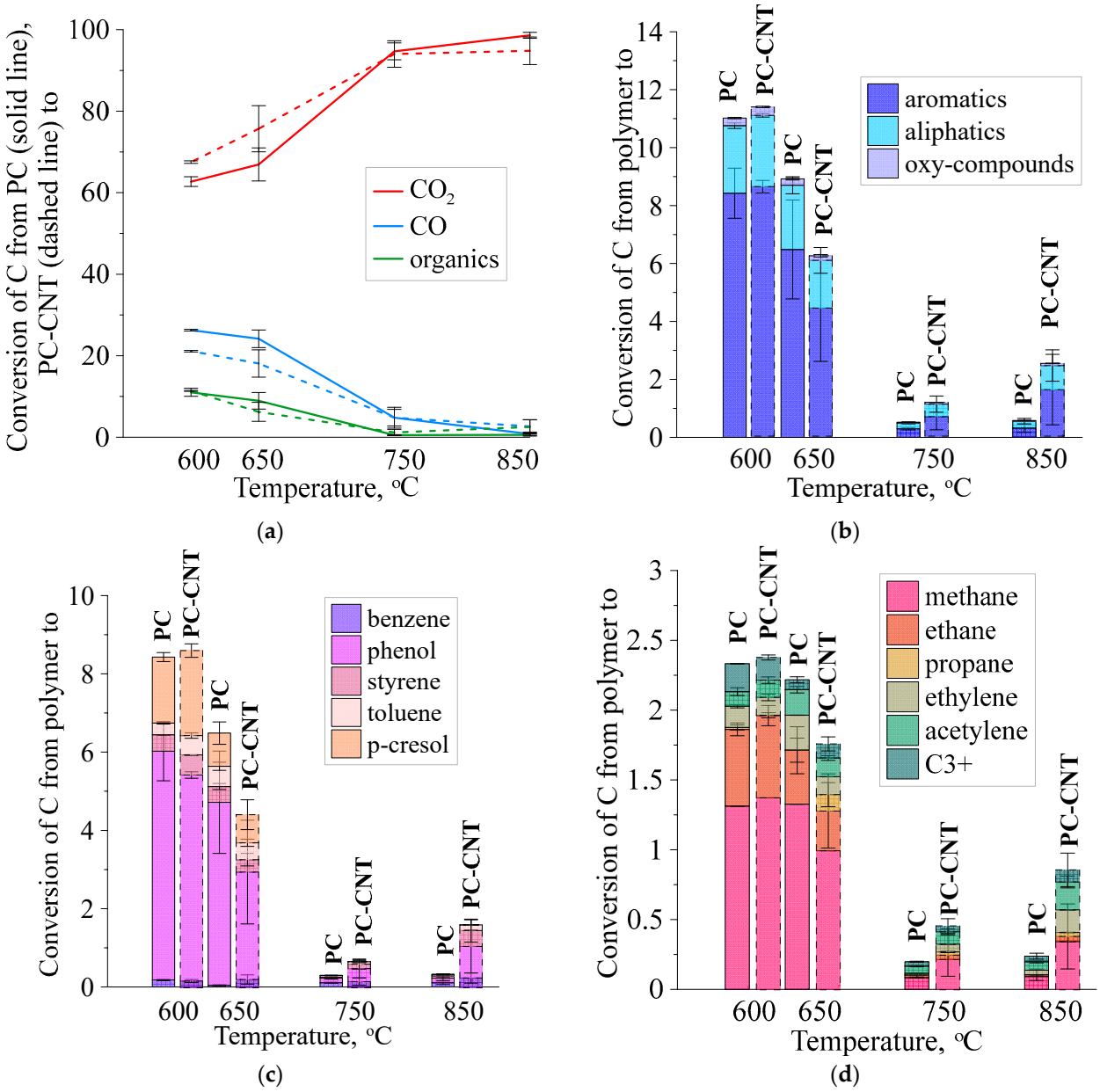

Figure 4. Composition of the PC and PC-CNT combustion in an inert fluidized bed formed by cenospheres: (**a**) main division into CO_2, CO, and organic compounds; (**b**) division of organic products into aromatic, aliphatic, and oxygenated derivatives; (**c**) share of individual organic products; (**d**) share of individual aliphatic products.

At low temperatures, 600–650 °C, in the inert fluidized bed (Figure 5a), the combustion of both PC and PC-CNT showed significant emissions of incomplete combustion products. In the bed heated to 600 °C, the conversion to CO_2 was only 62.7% for PC and 67.5% for PC-CNT. At this temperature, about one-third of the remaining gaseous products were organic compounds, and two-thirds were CO. When the temperature increased to 750 °C, the conversion to CO_2 for PC rose to 94.6%, and for PC-CNT to 94.8%. At the highest tested temperature (850 °C), both PC and PC-CNT demonstrated high conversion to CO_2, with values of 98.6% and 94.8%, respectively. It may appear that, in the range of 750 to 850 °C for PC-CNT, increasing the temperature does not lead to an increase in conversion. However, the error bars in Figures 4 and 5 indicate the average value for PC-CNTs is associated with a much greater fluctuation in concentrations compared to the combustion process of the PC. This suggests that the addition of CNTs may physically alter the heterogeneous combustion

of polycarbonate, e.g., as a result of the fact that the nanotube exposed to oxygen will burn more slowly than the polymer exposed to oxygen.

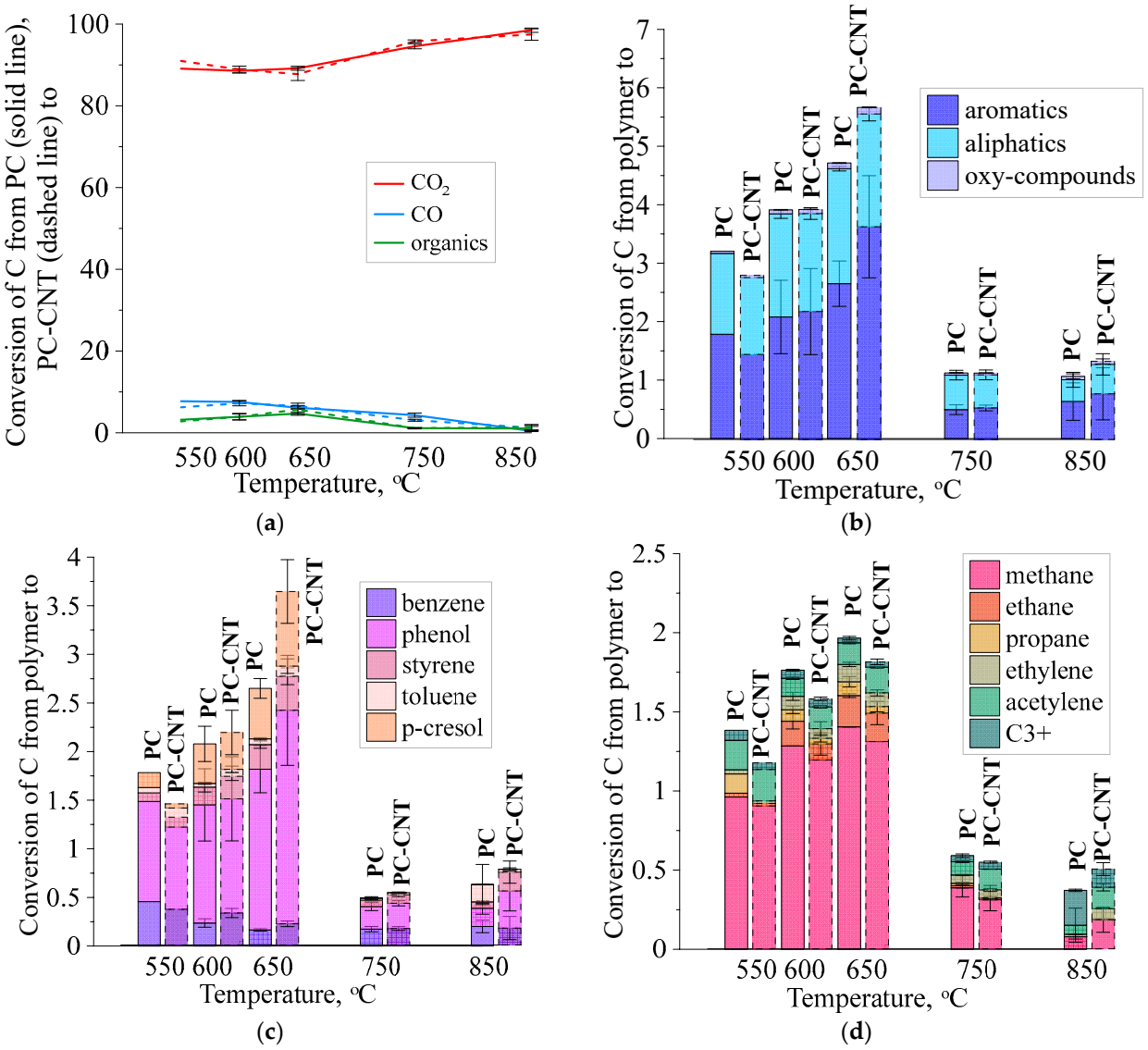

Figure 5. Composition of the PC and PC-CNT combustion in a catalytic fluidized bed formed by Fe_2O_3 cenospheres: (**a**) main division into CO_2, CO, and organic compounds; (**b**) division of organic products into aromatic, aliphatic, and oxygenated derivatives; (**c**) share of individual organic products; (**d**) share of individual aliphatic products.

If PC is burned, the contact surface between the polymer and the air is quite homogeneous in terms of the content of individual components, and hence small fluctuations in the combustion products. On the other hand, the combustion of PC-CNTs in a fluidized cenospheric bed leads to a contact surface between the particle and the air, which is much more complex and variable due to the presence of another material with different combustion characteristics. A higher temperature, 850 °C, can enhance these differences and cause heterogeneous combustion on a two-component surface (PC-CNT) to proceed with even higher fluctuations than at 750 °C.

The total share of organic compounds in the products of the combustion process of PC and PC-CNT in an inert fluidized bed appears to be comparable at each tested temperature. The influence of CNT primarily causes differences between CO and CO_2. The presence of CNT in PC-CNT helps achieve higher efficiency in the conversion of CO to CO_2 at lower

temperatures, up to 650 °C. As the temperature of the inert bed increases, the conversion of carbon in PC and PC-CNT to organic compounds decreases from 11% to 1% at 750 °C.

The use of the catalytic bed made of Fe_2O_3 cenospheres increased the combustion efficiency at low temperatures (Figure 5a). At 600 °C, 88.5% (for PC) and 88.9% (for PC-CNT) of the carbon was completely burned off. Based on these results, it was decided to lower the temperature of the catalytic fluidized bed by another 50 °C. At 550 °C, a total combustion efficiency of 89% for PC and 90% for PC-CNT was achieved. However, the time required for combustion at this temperature increased from 2 min to 25 min. While this result is chemically acceptable—since industrial installations have post-combustion stages—the extended combustion time is operationally unacceptable. This prolonged duration significantly impacts the overall efficiency and feasibility of the process in a practical industrial setting.

Higher combustion efficiencies in the catalytic fluidized bed reduced both CO and organic products of the process. At 600 °C, the conversion of carbon to CO and organic products was 7.5% and 3.9% for PC, respectively. For PC-CNT, the conversion rates were 7.2% and 3.9%, respectively. These values are approximately three times lower than those observed in the inert fluidized bed at the same temperature. While the results obtained in the inert bed showed a clear impact of CNT on the process products (Figure 4a), especially at low temperatures, the results for PC and PC-CNT on the catalytic bed are very similar (Figure 5a). This suggests that the influence of Fe_2O_3 on combustion efficiency is significantly greater than that of CNT.

The standard deviation values of the results obtained on the catalytic bed (Figure 5a) are significantly lower than those on the inert bed (Figure 4a). This increased repeatability is due to the change in the combustion mechanism. Besides being more efficient and repeatable, heterogeneous combustion is also safer. In this process, gas explosions in bubbles are eliminated, and the reaction occurs in the immediate vicinity of the catalyst grains.

The catalytic fluidized bed influences both the reduction in the proportion of organic products at various temperatures and their composition. On the inert fluidized bed (Figure 4b), aromatic compounds constitute the main organic fraction. Their share in organic products ranges from 76.5% and 75.8% for the combustion of PC and PC-CNT at 600 °C to 54.7% and 63.8% for the combustion of PC and PC-CNT at 850 °C. On the catalytic fluidized bed, the proportion of aromatics and aliphatic compounds is very similar (Figure 4b), indicating easier degradation of aromatic rings in the presence of Fe_2O_3. The main aromatic products are phenol and p-cresol on both the inert and catalytic fluidized beds (Figures 4c and 5c), while for aliphatic compounds, the main product is methane (Figures 4d and 5d).

5. Conclusions

It has been shown that the use of a fluidized bed made of a low-density material (which can be chemically inert or can have catalytic properties) promotes the proper organization of the combustion process of PC and PC-CNT. In such a process organization, in a fluidized bed made of cenospheres, it is possible to achieve high conversion rates to CO_2 amounting to 94.6% for PC and 94.8% for PC-CNT already at 750 °C without the need for additional gas afterburning systems. By using a fluidized catalytic bed in which a layer of Fe_2O_3 is deposited on the cenosphere, it is possible to increase the combustion efficiency at lower temperatures (600–650 °C) achieving a conversion to CO_2 of 88.5% for PC and 88.9% for PC-CNT compared to inert bed 62.7 for PC and 67.5% for PC-CNT. U/U_{mf} fluidization conditions in the range of 16–25 were applied, which ensured intensive mixing in the bed. As a result, a good supply of oxidizing agents was ensured to maintain the efficiency of PC and PC-CNT combustion. A difference has been observed between the combustion process in the catalytic and inert beds. If the fluidized bed layer has catalytic

properties, the fluctuations in the concentrations of combustion products decrease. It means that the layer plays an active role in the combustion of gaseous products formed in the heterogeneous process. Such an effect in other solutions (using a sand-fluidized bed) is achieved only through the use of the addition of secondary air and heating of the reactants in the freeboard zone.

In addition, simultaneous thermal analyses were performed to determine how a single particle behaves under conditions of elevated temperature and different concentrations of oxygen in a gaseous atmosphere. The results of the STA in the air atmosphere prove that the combustion processes of PC and PC-CNT take place in two stages. In the first stage, the addition of CNTs acts as barriers, limiting the availability of the oxidant to the polymer, causing (I) a lower degree of mass loss (65 mass%) compared to PC (70 mass%); (II) lower values of the maximum net instantaneous thermal effect (5.8 mW/mg) compared to PC (14.1 mW/mg); (III) lower total net exothermic effect (796 J/g) compared to PC (1294 J/g). In the second stage of combustion, CNT becomes an additional fuel, causing (I) a higher maximum of the net instantaneous thermal effect (23.1 mW/mg) compared to pure PC (12.5 mW/mg); (II) a higher total net thermal effect (up to 3900 J/g) compared to pure PC (2926 J/g).

The results of the STA under 2 vol.% O_2 conditions proved that the process of combustion of PC and PC-CNT under oxygen deficit (I) conditions requires a longer time and higher temperatures of 976 and 946 °C, respectively, for PC and CNT, compared to 692 and 693 °C for PC and PC-CNT in an atmosphere of 21 vol.% O_2; (II) the presence of a net instantaneous thermal effect of an endothermic nature as opposed to the decomposition in an atmosphere of 21 vol.% O_2, in which the material always release heat during combustion; (III) is associated with lower total net thermal effects of 3521 J/g PC and 3466 J/g PC-CNT compared to the atmosphere of 21 vol.% O_2 4220 J/g PC and 4696 J/g PC-CNT.

Author Contributions: Conceptualization, L.S.S., G.B.-P., W.Ż., Y.D. and I.H.; methodology, L.S.S., G.B.-P., W.Ż., Y.D., I.H., K.W. and D.T.; investigation, L.S.S., G.B.-P., W.Ż., Y.D., I.H., K.W. and J.W.; resources, L.S.S., Y.D., I.H., J.W. and D.T.; data curation, L.S.S., G.B.-P., W.Ż., Y.D. and I.H.; writing—original draft preparation, L.S.S. and G.B.-P.; writing—review and editing, L.S.S., G.B.-P. and W.Ż.; visualization, L.S.S. and G.B.-P.; supervision, W.Ż., I.H. and D.T.; project administration, L.S.S. and G.B.-P.; funding acquisition, W.Ż., I.H., J.W. and D.T. All authors have read and agreed to the published version of the manuscript.

Funding: This research received no external funding.

Data Availability Statement: The raw data supporting the conclusions of this article will be made available by the authors upon request.

Conflicts of Interest: The authors declare no conflicts of interest.

References

1. Davis, A.; Golden, J.H. Stability of polycarbonate. *J. Macromol. Sci. Part C* **1969**, *3*, 49–68.
2. Bendler, J.T. *Handbook of Polycarbonate Science and Technology*; CRC Press: Boca Raton, FL, USA, 1999.
3. Nishitsuji, S.; Watanabe, Y.; Ito, H.; Ishikawa, M.; Inoue, T.; Takenaka, M. Molecular weight dependence of the physical aging of polycarbonate. *Polymer* **2019**, *178*, 121571.
4. Raj, P.; Kumar, R. A Brief Review: Study on Mechanical Properties of Polycarbonate with Different Nanofiller Materials. In *Advances in Materials and Manufacturing Engineering: Select Proceedings of ICMME 2021*; Springer: Berlin/Heidelberg, Germany, 2021; pp. 285–291.
5. King, J.A. Synthesis of Polycarbonates. In *Handbook of Science and Technology*; MIT: Cambridge, MA, USA, 1999; pp. 23–42.
6. Al-Hakami, Y.M.N.; Wahab, M.A.; Yildirir, E.; Ates, F. Thermal degradation kinetics, thermodynamics and pyrolysis behaviour of polycarbonate by TGA and Py-GC/MS. *J. Energy Inst.* **2024**, *113*, 101499.
7. Charde, S.J.; Sonawane, S.S.; Sonawane, S.H.; Shimpi, N.G. Degradation kinetics of polycarbonate composites: Kinetic parameters and artificial neural network. *Chem. Biochem. Eng. Q.* **2018**, *32*, 151–165.

8. Połomska, J.; Żukowski, W.; Baron, J. Polycarbonate combustion in a fluidised bed reactor. *Proc. ECO Pole* **2011**, *5*, 87–96.
9. Komarov, F.F.; Mironov, A.M. Carbon nanotubes: Present and future. *Phys. Chem. Solid State* **2004**, *5*, 411–429.
10. Katoch, R.; Singh, R.S.; Patidar, R.D. Carbon Nanostructure Functionalization for Electromagnetic Shielding Applications. In *Handbook of Functionalized Carbon Nanostructures: From Synthesis Methods to Applications*; Springer International Publishing: Cham, Switzerland, 2024; pp. 1–38.
11. Zhang, J.; Panwar, A.; Bello, D.; Isaacs, J.A.; Jozokos, T.; Mead, J. The effects of recycling on the structure and properties of carbon nanotube-filled polycarbonate. *Polym. Eng. Sci.* **2018**, *58*, 1278–1284.
12. Kumar, S.; Prakash, R.; Murugan, S.; Singh, R.K. Performance and emission analysis of blends of waste plastic oil obtained by catalytic pyrolysis of waste HDPE with diesel in a CI engine. *Energy Convers. Manag.* **2013**, *74*, 323–331.
13. Saito, K.; Jehanno, C.; Meabe, L.; Olmedo-Martínez, J.L.; Mecerreyes, D.; Fukushima, K.; Sardon, H. From plastic waste to polymer electrolytes for batteries through chemical upcycling of polycarbonate. *J. Mater. Chem. A* **2020**, *8*, 13921–13926.
14. Brunelle, D.J. Polycarbonates. In *Encyclopedia of Polymer Science and Technology*; Wiley: Hoboken, NJ, USA, 2002.
15. Li, X.; Hristov, H.A.; Yee, A.H.; Gidley, D.W. Influence of cyclic fatigue on the mechanical properties of amorphous polycarbonate. *Polymer* **1995**, *36*, 759–765.
16. Awoyera, P.O.; Adesina, A. Plastic wastes to construction products: Status, limitations and future perspective. *Case Stud. Constr. Mater.* **2020**, *12*, e00330.
17. Zhao, X.; Korey, M.; Li, K.; Copenhaver, K.; Tekinalp, H.; Celik, S.; Kalaitzidou, K.; Ruan, R.; Ragauskas, A.J.; Ozcan, S. Plastic waste upcycling toward a circular economy. *Chem. Eng. J.* **2022**, *428*, 131928. [CrossRef]
18. Wielgosiński, G. Pollutant Formation in Combustion Processes. In *Advances in Chemical Engineering*; Nawaz, Z., Naveed, S., Eds.; InTech: Rijeka, Croatia, 2012; pp. 295–324.
19. Knox, A. *An Overview of Incineration and EFW Technology as Applied to the Management of Municipal Solid Waste (MSW)*; ONEIA Energy Subcommitte: Toronto, ON, USA, 2005.
20. Iannello, S.; Morrin, S.; Materazzi, M. Fluidised bed reactors for the thermochemical conversion of biomass and waste. *KONA Powder Part. J.* **2020**, *37*, 114–131.
21. Kwong, K.Y.; Marek, E.J. Combustion of biomass in fluidized beds: A review of key phenomena and future perspectives. *Energy Fuels* **2021**, *35*, 16303–16334.
22. Apaydin-Varol, E.; Polat, S.; Pütün, A. Pyrolysis kinetics and thermal decomposition behavior of polycarbonate-a TGA-FTIR study. *Therm. Sci.* **2014**, *18*, 833–842. [CrossRef]
23. Xu, F.; Wang, B.; Yang, D.; Hao, J.; Qiao, Y.; Tian, Y. Thermal degradation of typical plastics under high heating rate conditions by TG-FTIR: Pyrolysis behaviors and kinetic analysis. *Energy Convers. Manag.* **2018**, *171*, 1106–1115.
24. Moon, S.C.; Kim, J.Y.; Oh, B.T. Mechanical and flame resistant properties of polycarbonate-carbon nanotubes-ochre composites. *Polym. Eng. Sci.* **2014**, *54*, 1289–1299. [CrossRef]
25. Janhäll, S.; Petersson, M.; Davidsson, K.; Öman, T.; Sommertune, J.; Karedal, M.; Messing, M.E.; Rissler, J. Release of carbon nanotubes during combustion of polymer nanocomposites in a pilot-scale facility for waste incineration. *NanoImpact* **2021**, *24*, 100357.
26. Berkowicz-Platek, G.; Leski, K.; Żukowski, W.; Wrona, J. Processing of low-density waste in fluidized bed made out of lightweight expanded clay aggregate. *J. Clean. Prod.* **2022**, *349*, 131328. [CrossRef]
27. Antonakou, E.V.; Kalogiannis, K.G.; Stefanidis, S.D.; Karakoulia, S.A.; Triantafyllidis, K.S.; Lappas, A.A.; Achilias, D.S. Catalytic and thermal pyrolysis of polycarbonate in a fixed-bed reactor: The effect of catalysts on products yields and composition. *Polym. Degrad. Stab.* **2014**, *110*, 482–491.
28. Salah, L.S.; Ouslimani, N.; Chouai, M.; Danlée, Y.; Huynen, I.; Aksas, H. Predictive optimization of electrical conductivity of polycarbonate composites at different concentrations of carbon nanotubes: A valorization of conductive nanocomposite theoretical models. *Materials* **2021**, *14*, 1687. [CrossRef] [PubMed]
29. Han, M.S.; Lee, Y.K.; Kim, W.N.; Lee, H.S.; Joo, J.S.; Park, M.; Lee, H.J.; Park, C.R. Effect of multi-walled carbon nanotube dispersion on the electrical, morphological and rheological properties of polycarbonate/multi-walled carbon nanotube composites. *Macromol. Res.* **2009**, *17*, 863–869. [CrossRef]
30. Żukowski, W.; Berkowicz, G. The combustion of liquids and low-density solids in a cenospheric fluidised bed. *Combust. Flame* **2019**, *206*, 476–489. [CrossRef]
31. Castillo, F.Y.; Socher, R.; Krause, B.; Headrick, R.; Grady, B.P.; Prada-Silvy, R.; Pötschke, P. Electrical, mechanical, and glass transition behavior of polycarbonate-based nanocomposites with different multi-walled carbon nanotubes. *Polymer* **2011**, *52*, 3835–3845. [CrossRef]
32. Kashiwagi, T.; Du, F.; Winey, K.I.; Groth, K.M.; Shields, J.R.; Bellayer, S.P.; Kim, H.; Douglas, J.F. Flammability properties of polymer nanocomposites with single-walled carbon nanotubes: Effects of nanotube dispersion and concentration. *Polymer* **2005**, *46*, 471–481. [CrossRef]
33. Bourbigot, S.; Duquesne, S.; Jama, C. Polymer nanocomposites: How to reach low flammability? *Macromol. Symp.* **2006**, *233*, 180–190. [CrossRef]

34. Kashiwagi, T.; Grulke, E.; Hilding, J.; Groth, K.; Harris, R.; Butler, K.; Shields, J.; Kharchenko, S.; Douglas, J. Thermal and flammability properties of polypropylene/carbon nanotube nanocomposites. *Polymer* **2004**, *45*, 4227–4239. [CrossRef]
35. Bocchini, S.; Frache, A.; Camino, G.; Claes, M. Polyethylene thermal oxidative stabilisation in carbon nanotubes based nanocomposites. *Eur. Polym. J.* **2007**, *43*, 3222–3235. [CrossRef]
36. Gupta, R.; Singh, M.K.; Rangappa, S.M.; Siengchin, S.; Dhakal, H.N.; Zafar, S. Recent progress in additive inorganic flame retardants polymer composites: Degradation mechanisms, modeling and applications. *Heliyon* **2024**, *10*, e39662. [CrossRef]
37. Sabet, M.; Mohammadian, E. The inclusion of graphene nanoplatelet on the mechanical, thermal, and electrical characteristics of polycarbonate. *Polym. Bull.* **2023**, *80*, 2153–2169. [CrossRef]
38. Kim, Y.; Lee, S.; Yoon, H. Fire-safe polymer composites: Flame-retardant effect of nanofillers. *Polymers* **2021**, *13*, 540. [CrossRef]

Disclaimer/Publisher's Note: The statements, opinions and data contained in all publications are solely those of the individual author(s) and contributor(s) and not of MDPI and/or the editor(s). MDPI and/or the editor(s) disclaim responsibility for any injury to people or property resulting from any ideas, methods, instructions or products referred to in the content.